VICTORIA UNIVERSITY
MELBOURNE AUSTRALIA

Electrochemical characterisation of nanoparticulate zirconium dioxide-on-gold electrode for electrochemical detection in flow-based analytical systems

This is the Accepted version of the following publication

Accepted Manuscript

Electrochemical characterisation of nanoparticulate zirconium dioxide-on-gold electrode for electrochemical detection in flow-based analytical systems

Muhammed Ariful Islam, Mostafa A. Atia, Mirek Macka, Brett Paull, Parvez Mahbub

Electrochemical characterisation of nanoparticulate zirconium dioxide-on-gold electrode for electrochemical detection in flow-based analytical systems
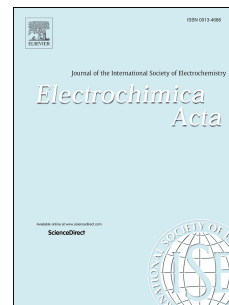
Muhammed Ariful Islam [a], Mostafa A. Atia [a], Mirek Macka [a, b, c], Brett Paull [a, d], Parvez Mahbub [a, e, *]

[a] Australian Centre for Research on Separation Science (ACROSS), School of Natural Sciences, University of Tasmania, Private Bag 75, Hobart 7001, Australia

[b] Department of Chemistry and Biochemistry, Mendel University in Brno, Zemedelska 1, CZ-613 00 Brno, Czech Republic

[c] Central European Institute of Technology, Brno University of Technology, Purkynova 123, CZ-612 00 Brno, Czech Republic

[d] ARC Training Centre for Portable Analytical Separation Technologies (ASTech), School of Natural Sciences, University of Tasmania, Private Bag 75, Hobart 7001, Australia

[e] Institute for Sustainable Industries and Liveable Cities, Victoria University, Footscray Park Campus, Melbourne 3011, Australia

* Email: parvez.mahbub@utas.edu.au

Highlights

- Electrochemical characterisation of nanoparticulate ZrO_2-on-Au is investigated for flow-based analysis.

- Electrochemical reversibility and 100% increase of effective surface area are achieved in ZrO_2-Au.

- LODs of ascorbic acid, 2,3-dihydroxybenzoic acid, and pyrocatechol are the lowest achieved to-date.

- Stability of ZrO_2-Au electrode in continuous-flow system is the highest reported to-date (8.5 hr).

Graphical abstract
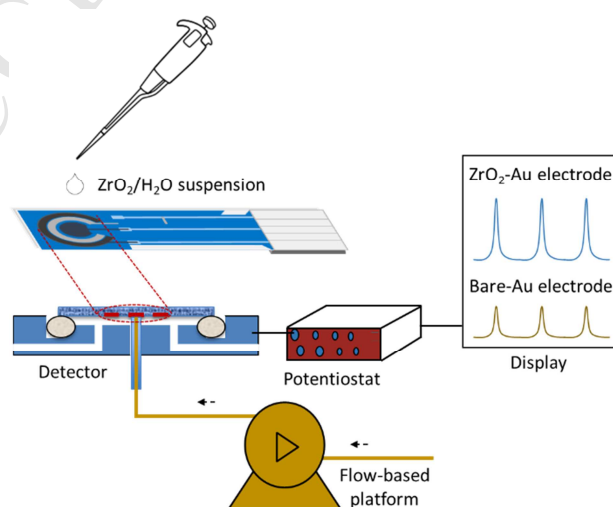
Abstract

The modification of gold (Au) electrode using zirconium dioxide nanoparticles (ZrO$_2$ NPs) has been investigated for enhanced electrochemical (EC) detection in flow-based analytical systems. The average size of ZrO$_2$ NPs deposited in a facile procedure on the Au electrode surface was calculated as 22.5±7 nm. Redox behaviour of a test solute, ferrocyanide [Fe(CN)$_6$]$^{4-}$, on the bare- and ZrO$_2$-Au electrodes was initially investigated using cyclic voltammetry. From the voltammograms of bare- and ZrO$_2$-Au electrodes, the EC reversibility values and effective surface area were experimentally determined for the first-time in this study. Further, EC reversibility and 100% increase in effective electrode surface area were confirmed in ZrO$_2$-Au electrode through investigating the detection response (current). The EC performance of the ZrO$_2$-Au electrode was then investigated in amperometric detection of selected electroactive solutes separated by reversed-phase HPLC. The limits of detection (LODs), based upon an injection volume of 10 µL for ascorbic acid, 2,3-dihydroxybenzoic acid and pyrocatechol were 0.09 µM, 0.04 µM, and 0.10 µM, respectively (RSD 2.5 %, n= 9, r^2 = 0.99 for concentration range 1-100 µM). These LODs for the ZrO$_2$-Au electrode were 2-times lower for 2,3-DHBA, and pyrocatechol than the lowest LODs reported in the literature for EC detection in HPLC. The ZrO$_2$-Au electrode demonstrated satisfactory repeatability of preparation, detection reproducibility and high stability (8.5 hr) during continuous-flow in FIA and 45 days during intermittent use with HPLC, at flow rate of 0.6 mL min^{-1}. This work has demonstrated a comprehensive EC characterisation of Au electrode with nanoparticulate ZrO$_2$ for flow-based analytical systems.

Keywords

Electrochemical detection

Flow-based analytical systems

Nanomaterials

Zirconium dioxide

Abbreviations

2,3-DHBA   2,3-dihydroxybenzoic acid

ACN   Acetonitrile

AD   Amperometric detection

CV   Cyclic voltammetry

EC   Electrochemical

FC   Flow cell

$[Fe(CN)_6]^{4-}$ Ferrocyanide

LODs   Limits of detection

NMs   Nanomaterials

NPs   Nanoparticles

S/N   Signal-to-noise ratio

SEM   Scanning electron microscopy

TEM   Transmission electron microscopy

WE   Working electrode

ZrO_2 Zirconium dioxide

1. Introduction

The use of nanomaterials (NMs) [1-7] as electrode surface modifiers for enhanced electrochemical (EC) detection, has become one of the hottest fields of research in electroanalytical chemistry. The increasing interest in NMs is driven by their unique chemical and physical properties [2, 8]. For example, metal NMs act as electrocatalysts by decreasing the overpotential of many EC reactions and increasing the electrical conductivity of modified surfaces by enhancement of faster transfer of electrons in EC analysis [2, 8, 9]. Kleijn *et al.* [10] also reported the use of NMs on electrode surface resulting in an increased rate of mass-transport to the electrode surface via the formation of diffusion layers above each NP or NPs agglomerates. These properties make them extremely suitable for augmenting the performance of EC detection in terms of larger effective surface areas and better EC response (in terms of peak current, EC reversibility, and EC conversion efficiency) [2], including when used within flow-based analytical platforms, such as flow injection analysis (FIA), capillary electrophoresis, and high-performance liquid chromatography (HPLC) [11, 12]. The most reported NMs used for electrode modification in flow-based analytical systems have been silver (Ag) [2], gold (Au) [2, 13, 14], nickel (Ni) [15, 16], platinum (Pt) [2], boron (B)-doped

diamond [17-19], iron (Fe) oxide-reduced graphene oxide [13, 20], and manganese (Mn) dioxide [2]. These materials are widely used due to their high electrical conductivity (Ag > Au > Ni > Fe > Pt > Mn > B [21]) as well as due to the inert properties.

The drawbacks associated with the use of NMs for conventional or disposable electrode modification process include time consuming multiple steps in modification techniques such as electrodeposition [13, 16] and sol-gel processes [22, 23], the requirement of polishing the electrode surface before modification [13, 14, 24], the use of reagents to enhance the porosity of the electrode surface [25], the requirement of technical skills for modification [13, 16, 22, 23], and the limited stability of the modified electrode surface, usually 5-7 days [26, 27]. Most recent reports on the preparation and/or modification of electrodes with NMs have drawbacks such as use of large quantities of NMs (e.g. *ca.* 965 mg in [24]) together with expensive modification techniques [7, 13-17, 22, 23, 25]. Further, to-date the EC reversibility, effective surface area, and stability of the NMs modified-electrode surface in continuous-flow has not been experimentally investigated [7, 28], and the often limited stability of modified-electrode surfaces [26, 27] significantly hinders the potential of using modified-electrodes in flow-based analytical systems [7, 13, 28-30]. Therefore, the integration of disposable electrodes with flow-based analytical systems requires accurate characterisation of bare and modified surface areas in terms of current, EC reversibility, effective surface area, and stability of the modified-electrode surface in continuous-flow as well as intermittent use within an analytical platform.

In this context, zirconium dioxide nanoparticles (ZrO_2 NPs) have been reported in the literature as electrocatalyst [9, 28, 30-38] for use in EC techniques in stopped-flow mode such as cyclic voltammetry (CV), linear sweep voltammetry, and differential pulse voltammetry , particularly due to the ZrO_2 NPs' stability upon the modified electrode surface [28, 30, 34], good electrical conductivity (Pt > Zr > Mn [21]), high strength and resistance to fracturing, high melting point, low thermal conductivity and high corrosion resistance, as well as the fact that the ZrO_2 NPs are non-toxic [28, 37]. In 2017, Mohammadizadeh *et al.* [28] reported ZrO_2 NPs-modified porous graphite surfaces with a better EC response for the determination of propranolol using CV, LSV, and DPV. In 2015, Gholivand *et al.* [38] proposed a new electrode composed of a ZrO_2 NPs carbon-paste electrode modified with 3-(4'-amino-3'-hydroxybiphenyl-4-yl)-acrylic acid for the determination of hydrazine in aqueous solutions using CV. In 2013, Mazloum-Ardakani *et al.* [9] prepared a mobil crystalline material/ZrO_2 NPs-modified carbon-paste electrode that required no additional electron transfer mediator or reagent, for simultaneous and selective CV determination of

epinephrine and acetaminophen. Some interesting applications of ZrO_2 NPs in different research fields have been reported such as their use as catalysts in gas-sensing, use in photocatalysis, wastewater treatment, and as stable column packing materials for elevated temperatures [28, 32-35]. However, to-date there have been no reports of using ZrO_2 NPs-modified electrodes for EC detection in analytical flow techniques (such as HPLC and FIA). The use of low-cost ZrO_2 NPs to modify disposable electrodes [22, 39] can be beneficial in terms of a rapid modification process (approx. 10 min) for the formation of the porous electrode surface that can provide a larger electro-active surface area for an enhanced EC response (current) [9, 28, 30, 38] and facilitate reversible (Nernstian) EC reaction [28, 40, 41]. In addition, the use of ZrO_2 NPs can increase the stability and corrosion resistance [28, 37] properties of the electrode in flow-based analysis.

Therefore, the aim of this study was to investigate EC detection using disposable Au electrode modified with ZrO_2 NPs (termed here as ZrO_2-Au) within flow-based analytical systems. We also aimed to demonstrate the enhanced EC performance using CV in terms of peak current, resulting EC reversibility and effective surface area. Additionally, we demonstrated enhanced amperometric response (current) using the disposable ZrO_2-Au electrode with a miniaturised EC detector coupled to an HPLC for detection of electroactive analytes including ascorbic acid (considered as an antioxidant [42]), 2,3-dihydroxybenzoic acid (2,3-DHBA, a biological marker for the detection and quantification of $OH^{\bullet}$ radicals [43]), and pyrocatechol (a possible human carcinogen classified by International Agency for Research on Cancer (IARC) [44]). The stability test of ZrO_2-Au electrode is also investigated for continuous-flow in FIA and intermittent use in HPLC.

2. Experimental

2.1 Chemicals

Analytical grade standards and reagents were used in this study. These were potassium ferrocyanide trihydrate ($K_4Fe(CN)_6.3H_2O$, Ajax, Australia), potassium chloride (KCl, Sigma-Aldrich, Sweden), ascorbic acid, 2,3-dihydroxybenzoic acid (2,3-DHBA), pyrocatechol, citric acid, sodium citrate dihydrate (Sigma-Aldrich, USA), acetonitrile (ACN, 99.8% HPLC grade, VWR, Australia), and milli-Q water (Millipore, USA). HPLC grade solvents were used for all separations. All test solutes and mixtures were freshly prepared in ACN and citrate buffer which was used as HPLC mobile phase. The suspension of ZrO_2 NPs (10 wt. % in H_2O, Sigma-Aldrich, USA) was used for preparation of ZrO_2-Au electrode.

2.2 Instrumentation

A simple CV platform was assembled using a uProcess (LabSmith™, USA) microfluidic system. The platform consisted of two programmable microsyringe pumps (model: SPS01) with 100 µL glass syringes, one four port valve ('L' pattern flow, and a two-position switching valve, model: AV201-C360). All pumps and switching valves were connected via PEEK tubing (Polyether ether ketone, 150 µm i.d., 360 µm o.d.) on a uProcess™ Breadboard. The software uProcess™ was used for controlling the various components and the volumetric flow rate of the microsyringe pumps [45]. A polyimide coated fused silica capillary (100 µm i.d., 360 µm o.d., length 7 cm, TSP100375, Polymicro Technologies™, USA) was used to connect the switching valve and the EC detector gap flow cell (gap-FC) [12]. The full instrumental scheme is shown in the SI (see **Error! Reference source not found.**).

The HPLC (Alliance Waters 2690, Waters, USA) consisted of an injector valve (SM4, Waters, USA), a thermostatted reversed-phase (RP) column (YMC Pac Pro C18, length 25 cm x i.d. 4.6 mm, pore size 5 µm, YMC Co. Ltd, Japan), and an UV detector (model: 996 PDA detector, path length: 10 mm, cell volume: 8 µL, Waters, USA). The HPLC was operated by Empower software (Waters, USA). The gap-FC was coupled to HPLC as illustrated in SI **Error! Reference source not found.**. In UV detector, we have observed a higher signal (peak height) at 254 nm for ascorbic acid, and at 280 nm for 2,3-DHBA, pyrocatechol, and dopamine. Therefore, we used both 254 nm and 280 nm for UV detection in this study.

The EC detection in both CV and HPLC configurations was performed using the commercially available screen-printed electrodes of dimensions: length 25.40 x width 7.26 x height 0.63 ± 0.05 mm (model: sensor $AC_1W_2R_S$, BVT Technologies, Czech Republic). The electrode consisted of a Au working electrode (diameter: 2 mm), a Ag reference electrode, and a Pt auxiliary electrode. Further details of electrode materials and fabrication can be found in recent reviews by Li *et al.* [39] and Couto *et al.* [22]. A potentiostat (model ER466CE, eDAQ Pty Ltd, Australia) was connected to the gap-FC and operated with eDAQ software (eDAQ Pty Ltd, Australia) to perform EC detection. Transmission electron microscopy (TEM, model: HT7700, Hitachi, Japan) and scanning electron microscopy (SEM, model: Hitachi SU70, Hitachi, Japan) were utilised for characterising the modified electrode surface in terms of size distribution and morphology of ZrO_2 NPs in this study.

2.3 Modification of electrode

The bare-Au surface was rinsed thoroughly with water and dried with inert nitrogen gas. The surface of the Au was coated with 10 μL aliquot of the filtrated ZrO_2 NPs/H_2O suspension (10 wt. % in H_2O) and the solvent was allowed to evaporate for approx. 10 min at room temperature 20 °C. The ZrO_2 NPs were attached to the electrode surface by physical adsorption (i.e. weak Van der Waals forces) [46].

2.4 ZrO_2 NPs size distribution

The TEMs of ZrO_2 NPs (see SI **Error! Reference source not found.**) and SEMs of bare- and ZrO_2-Au electrodes surface (see SI **Error! Reference source not found.**) are given in SI. The histogram illustrated in SI **Error! Reference source not found.** shows a Gaussian distribution of size (diameter) of ZrO_2 NPs. The mean diameter of ZrO_2 NPs was calculated to be 22.5±7 nm using a Gaussian model (Origin 2016, OriginLab Corporation, USA) from the histogram. The resulting 22.5±7 nm diameter of ZrO_2 NPs confirmed that the agglomeration effect of ZrO_2 NPs from the ZrO_2/H_2O suspension on Au surface was insignificant. The porosity, as defined in [47, 48], was calculated by measuring particle density [49] and bulk density of ZrO_2 NPs [50] (approx. 94.5 %, for detail calculation see SI section **Error! Reference source not found.**). The formation of porous surface by the ZrO_2 NPs was also observed in SEM (see SI **Error! Reference source not found.**).

3. Results and discussions

Initially, CV was performed to study the EC behaviour of species involved in redox (reduction and oxidation) reactions at electrodes [51]. From voltammograms of bare- and ZrO_2-Au electrodes, the peak current, EC reversibility, and effective surface area are compared in the following section. This investigation was undertaken prior to demonstrating the analytical application of ZrO_2-Au electrode in FIA and HPLC for enhanced EC detection of target solutes. The AD in FIA and HPLC was performed under optimised conditions reported in Islam *et al.* [12], with a flow rate of 0.6 mL min^{-1}, capillary i.d. 100 μm (UV-gap FC), and a gap distance (capillary outlet-electrode) of 30 μm. Additionally, the optimised applied potential +800 mV was obtained for ZrO_2-Au electrode in terms of signal-to-noise (S/N, see SI **Error! Reference source not found.**).

3.1 Cyclic voltammetry

The peaks response (current) for the EC redox behaviour of potassium ferrocyanide at bare- and ZrO_2-Au electrodes are shown in Fig. 1. The redox peak currents of ±50 μA at ±160 mV obtained for the bare-Au, which were *ca.* 100%

increased to ±100 μA at ±185 mV for ZrO$_2$-Au electrode with the same scan rate of 700 mV s^{-1}. In our study, the use of ZrO$_2$ NPs on Au electrode increased the electrical conductivity of modified surfaces via faster transfer of electrons. We also attribute this increase of peak current to the formation of a porous electrode surface that increased the electro-active surface area, and facilitated reversible (Nernstian) EC reaction [28, 40, 41].

EC reversibility can be achieved when the redox reaction is at equilibrium, no side reactions take place and electron transfer kinetics are fast to keep the surface concentrations of redox-active species at certain values expected by the Nernst equation [40]. Nie *et al.* [40] suggested EC reversibility as the difference in peak potentials as shown in equation 1.

$$\Delta E_P = E_{P_c} - E_{P_a} = \frac{59}{n} \qquad (1)$$

where, ΔE_P (in mV) = difference in peak potentials, E_{P_a}= anodic peak potential, and E_{P_c}= cathodic peak potential, and n= the number of electrons transferred.

From equation 1, the complete EC reversibility can be achieved when ΔE_P= 59 mV (when, n= 1 in this study). We observed E_{P_a} and E_{P_c} from Fig. 1 and calculated ΔE_P of [Fe(CN)$_6$]$^{4-}$ for bare- and ZrO$_2$-Au electrodes as *ca.* 10 mV and 59 mV, respectively (where, n = 1) by employing equation 1. This evaluation of peak potentials shows that a complete EC reversibility was achieved by using ZrO$_2$-Au electrode (where, ΔE_P = 59 mV). We attribute the increase of ΔE_P values from 10 mV to 59 mV by using ZrO$_2$ NPs for the formation of porous electrode surface.
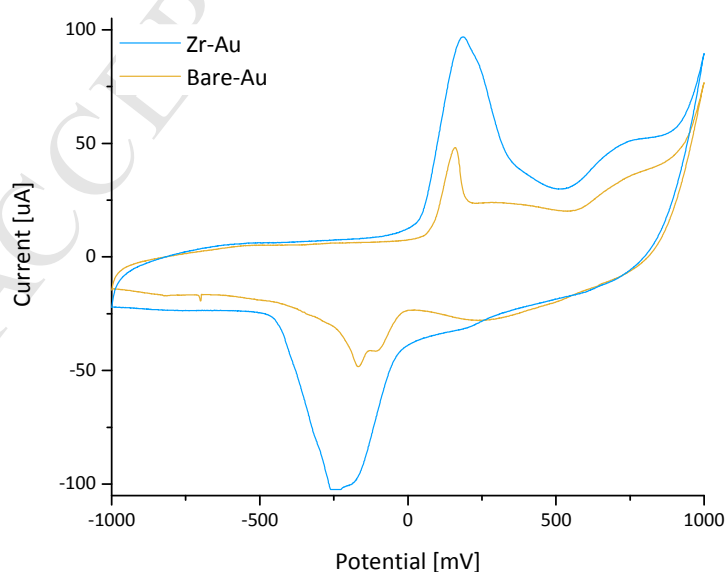
Fig. 1. The cyclic voltammogram of 100 µM $[Fe(CN)_6]^{4-}$ in 0.1 M KCl at a scan rate 700 mV s^{-1} for bare- and ZrO$_2$-Au electrodes. The voltammogram for the EC redox reaction of $[Fe(CN)_6]^{4-}$ was investigated from -1 V to 1 V at scan rates 10-800 mV s^{-1} (see SI **Error! Reference source not found.**). Two overlaid cathodic peaks were observed due to the presence of impurities in KCl (see further explanations of overlaid cathodic peaks in SI **Error! Reference source not found.**).

In the reversible redox analysis, we observed the different peak current at bare- and ZrO$_2$-Au electrode for same geometrical surface area of electrode (*ca.* 2 mm^2 in this study). Therefore, the effective surface area [52, 53] of bare- and ZrO$_2$-Au electrodes were calculated using the Randles-Sevcik equation (equation 2) [25, 54-56] for a reversible redox analysis.

$$i_p = 269\ ACn^{3/2}D^{1/2}v^{1/2} \qquad (2)$$

where, i_p = peak current [A], A = effective surface area [mm^2], C = concentration [mM], D = diffusion coefficient [cm^2 s^{-1}], and v = potential scan rate [V s^{-1}].

The peak current for the EC redox reaction of $[Fe(CN)_6]^{4-}$ was investigated over a wide range of potential scan rates from 10 to 800 mV s^{-1} (see SI **Error! Reference source not found.**). The anodic peak currents reflected the oxidation of $[Fe(CN)_6]^{4-}$ to $[Fe(CN)_6]^{3-}$, and were measured at +160 mV. The plots of current vs. square root of scan rate for both bare- and ZrO$_2$-Au electrodes are illustrated in Fig. 2.
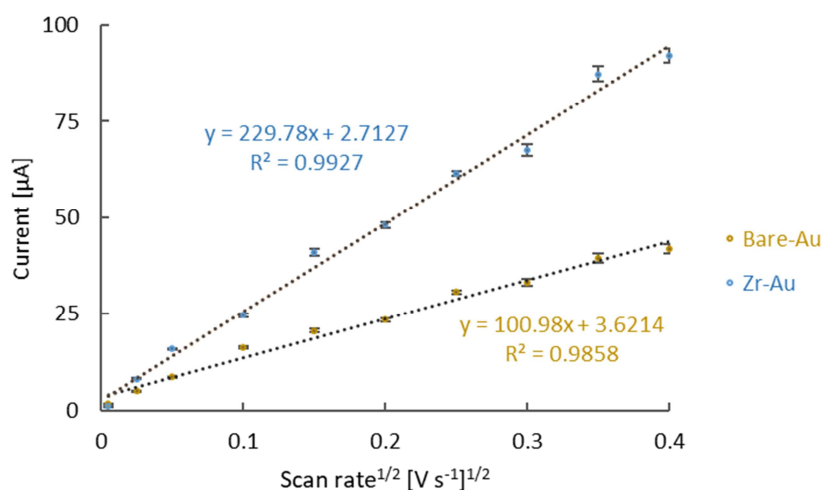

Fig. 2. Anodic peak current of 100 µM $[Fe(CN)_6]^{4-}$ in 0.1 M KCl for bare- and ZrO$_2$-Au electrodes. Conditions: peak current measured at +160 mV and potential scan rate ranging from 10 to 800 mV s^{-1} (n= 3). At zero scan rate, charging current resulting from the double layer effects [57, 58] was observed during the measurement.

The resulting peak current for the reversible redox analysis can be defined by Equation 2. According to the equation, the magnitude of peak current has a linear dependence on the concentration of the test solute and the square root of the potential scan rate. Here, a linear fit with A equal to slope/$269Cn^{3/2}D^{1/2}$ was obtained [25] for the test solute, 100 μM [Fe(CN)$_6$]^4. A was calculated to be 135 mm^2 and 270 mm^2 for bare- and ZrO$_2$-Au electrodes, respectively (where, slope (i_p [A]/$v^{1/2}$[V s^{-1}])= 0.0001 for bare-Au and 0.0002 for ZrO$_2$-Au electrode in **Error! Reference source not found.**, C= 100 μM (i.e., 0.1 mM) [Fe(CN)$_6$$^{4-}$], n= 1, and diffusion coefficient, $D^{1/2}$= 0.0027 cm^2 s^{-1} [25, 54-56]). The results obtained for the ZrO$_2$-Au electrode indicates a 100% increase of A which is due to the presence of ZrO$_2$ NPs on the surface of the Au. Importantly, the changes in effective surface area of using modified electrode is experimentally determined for the first time amongst the reported EC detection studies to-date [9, 28, 38]. This investigation also showed the resulting current obtained in EC detection is influenced by the effective surface area rather than the geometrical surface area of electrode. The comparison between voltammograms of bare- and ZrO$_2$-Au electrode (see Fig. 1 and **Error! Reference source not found.**) demonstrates the beneficial effect of ZrO$_2$ for the enhanced EC response of target solutes (such as ascorbic acid, 2,3-DHBA, and pyrocatechol in this study) by minimising the capacitance of double layer [59, 60] (see SI section 3.2). These characterisations can be beneficial specially for miniaturised flow-based analytical systems (such as μFIA-EC and capillary-LC-EC, see our previous work [12]), where ZrO$_2$-Au can provide enhanced EC signal (current) to overcome the limitations of measuring effective cell volume and EC conversion efficiency, when flow rate < 0.1 μL min^{-1}.

3.2 HPLC-UV-EC

In this study, the analytical application of ZrO$_2$-Au electrode was investigated for enhanced EC detection of test solutes, namely ascorbic acid, 2,3-dihydroxybenzoic acid and pyrocatechol. Under optimised conditions, the chromatograms of test solutes using ZrO$_2$-Au electrode in HPLC are illustrated in Fig. 3. The calibration curves for both UV and EC detection were plotted using peak heights for each solute (see SI **Error! Reference source not found.**). There was a significant difference observed in the limits of detection (LODs) obtained using UV and EC detection. The LOD values from EC detection were approx. 4-49 times lower than those obtained with UV detection at 254 nm and 280 nm. The LODs obtained for the AD using the ZrO$_2$-Au electrode were 0.09 μM, 0.04 μM, and 0.10 μM for ascorbic acid, 2,3-DHBA, and pyrocatechol, respectively (see Table 1, n= 9, determination coefficient r^2= 0.99 for 1-100 μM). Furthermore, the LODs obtained using the ZrO$_2$-Au electrode in a HPLC-EC system are comparable

with the lowest reported for EC detection in flow-based analytical systems. The calculated LODs are about 2-times lower than the lowest reported LODs in our previous work [12] for 2,3-DHBA, and pyrocatechol as illustrated in Table 1. In this study, we observed 95 to 180-times improvement of current at 800 mV while comparing the voltammograms of solutes (ascorbic acid, 2,3-DHBA, and pyrocatechol, see SI **Error! Reference source not found.**) using bare- and ZrO_2-Au electrode. The results from Table 1 also provide a significant reduction (*ca.* 3-times) of the baseline noise and enhanced peak efficiency *ca.* 4-8% compared to reported EC detection in flow-based analytical systems [12] for all solutes, namely ascorbic acid, 2,3-dihydroxybenzoic acid and pyrocatechol.

The Student's t-test and F-test were conducted to express confidence intervals of LODs in our study compared with HPLC-AD work reported by Pluangklang *et al.* [61]. The value of t-test and F-test were calculated using the equations (see SI section **Error! Reference source not found.**) given by Harris [34]. The calculated confidence level ranged from 90 to 95% for 2,3-DHBA, and pyrocatechol. The F-test resulted two standard deviations are significantly different for 2,3-DHBA (where, $F_{calculated}$ 4.3 > F_{table} 3.39), however the difference is insignificant for pyrocatechol ($F_{calculated}$ 3.09 < F_{table} 3.39).

The performance of gap-FC in terms of peak asymmetry, peak efficiency and peak FWHM were also compared with a UV detector in this platform (see Table 1). The delay time between chromatograms for UV and EC detection in this study were 4.9-5 s, the peak efficiency decreased 1.5-6% in EC detection and approx. 2.5% peak broadening was also observed for the EC detector. We attribute these insignificant differences in peak efficiency and broadening in EC detector due to the connecting pathways [62], geometry [63] and effective volume of the FC [34]. EC detection in our previous studies also reported minor differences in peak efficiency and broadening compared to the UV detection [12].
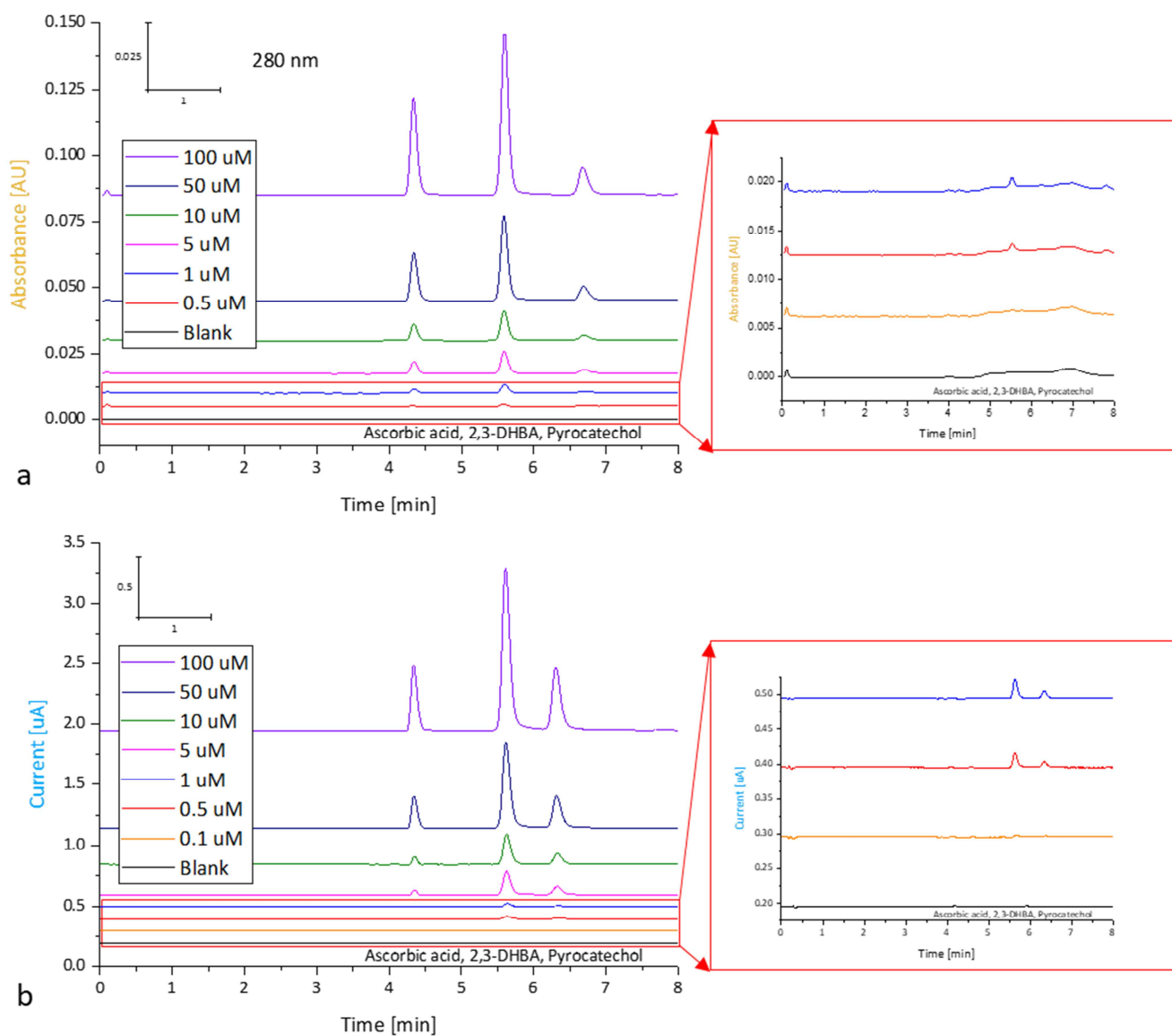
Fig. 3. Chromatograms showing separations of ascorbic acid, 2,3-DHBA, and pyrocatechol using a HPLC (a. UV detection, and b. EC detection). Conditions: mobile phase (v/v= 60:20:20): ACN: water:25 mM citrate buffer (pH 3.5), elution: isocratic, flow rate: 0.6 mL min^{-1}, sample injection volume: 10 µL, HPLC column (injector-UV detector): YMC Pac Pro C18 reversed-phase column (length: 25 cm, i.d: 4.6 mm, particles size: 5 µm), column oven temperature: 25 ^{o}C, pressure: *ca.* 1050 psi (73 bar), capillary (UV-gap-FC) i.d: 100 µm (length: 7 cm), gap distance: 30 µm, WE: ZrO$_2$-Au, potential: +800 mV. UV absorbance wavelength: 254 nm (see SI **Error! Reference source not found.**) and 280 nm.

Table 1. Comparison of the analytical performance of EC and UV detection in a HPLC. *

Detector (WE)	Analyte	Void Volume [a] [mL]	Peak asymmetry factor [b]	Peak efficiency (plate number [c]/ column length) [N m^{-1}]	Peak FWHM [min]	Baseline noise (SD)	LOD [d] [μM]	RSD [%]	Sensitivity [e]	Ref.
UV	Ascorbic acid	0.1	1.1-1.3	39900-62000	0.12-0.16	0.07 [mAU] (254 nm)	0.37	1.1-4.8	1.9	This work
	2,3-DHBA						0.83		0.6	
	Pyrocatechol					0.05 [mAU] (280 nm)	4.90		0.1	
EC (Pt)	Ascorbic acid	-	1.0-1.2	36000-55500	0.10-0.13	0.5 [nA]	0.10	1.3-4.9	15.9	[12]
	2,3-DHBA						0.09		17.8	
	Pyrocatechol						0.20		8.1	
EC (ZrO$_2$-Au)	Ascorbic acid	-	1.2-1.3	39300-58000	0.09-0.13	0.16 [nA]	0.09	1.6-2.8	5.5	This work
	2,3-DHBA						0.04		13.4	
	Pyrocatechol						0.10		5.1	

* Solvent (v/v): 25 mM citrate buffer, pH 3.5:ACN (20:80), flow rate: 0.6 mL min^{-1}, and applied potential: 800 mV.

[a] Void volume calculated by multiplying flow rate and the elution time for mobile phase or unretained solute when the first baseline disturbance is observed [34].

[b] Peak asymmetry factor, $A_s = \frac{w_R}{w_L}$, where w_R is the distance from the peak midpoint (perpendicular from the peak highest point to baseline) to the trailing edge of the peak and w_L is the distance from the leading edge of the peak to the peak midpoint measured at 10 % of peak height [34].

[c] Plate number, $N_P = 5.54 \left(\frac{t_R}{w_{h/2}}\right)^2$, where t_R is retention time and $w_{h/2}$ is width of the peak at half height [34].

[d] LODs were calculated by dividing the three-times of standard deviation (SD) of a blank response (noise level) by the slopes of the corresponding calibration curves [34]. In UV detection, LODs calculated at 254 nm for ascorbic acid and 280 nm for 2,3-DHBA, and pyrocatechol.

[d] Sensitivity was calculated from 0.1 to 100 μM in this study (0.5-100 μM in our previous work [12]). The sensitivity units are mAu μM^{-1} (UV detection) and nA μM^{-1} (EC detection).

3.3 Stability tests

The stability of the ZrO$_2$-Au electrode surface was tested in FIA and HPLC at room temperature (*ca.* 20 $^{\circ}$C). In the FIA platform (see Fig. 4), 100 µM of 2,3-DHBA was continuously injected at flow rate 0.6 mL min^{-1} (50 injections, with 10 min analysis time per injection). It was observed that the ZrO$_2$-Au electrode was stable for 8.5 hr at 0.6 mL min^{-1} (RSD *ca.* 2.6%) in continuous-flow. Most EC measurements reported stability of modified electrodes ranging ca. 5-7 days [26, 27]. However, there are no reports on stability of modified electrodes when used in continuous-flow modes such as in FIA to date. The analysis time reported in EC detection in continuous flow modes using FIA ranged up to ten minutes [11, 64]. As our measured stability of the modified electrode was significantly higher than those reported in previous studies [11, 64], we did not continue the stability test in continuous mode beyond 8.5 hours in FIA.
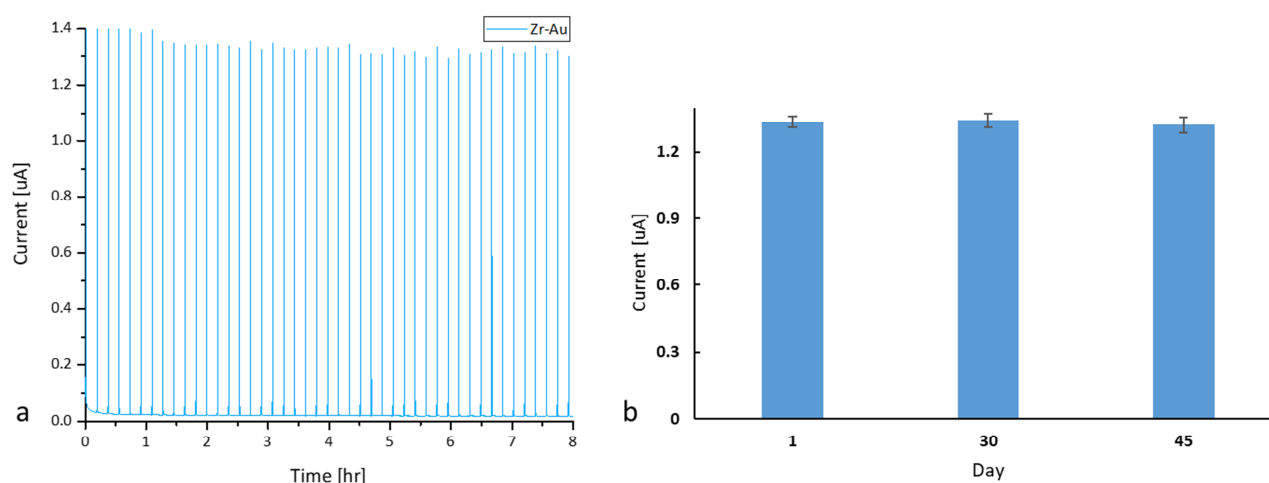

Fig. 4. Stability test of ZrO$_2$-Au electrode (a) continuous-flow in FIA and (b) intermittent use with HPLC. Conditions (a): solute: 100 µM 2,3-DHBA, mobile phase (v/v= 60:20:20): ACN:water:25 mM citrate buffer (pH 3.5), elution: isocratic, flow rate: 0.6 mL min^{-1}, sample injection volume: 1 µL, capillary (UV-gap-FC) i.d: 100 µm (length: 7 cm), gap distance: 30 µm, WE: ZrO$_2$-Au, potential: +800 mV. Conditions (b): same conditions for 2,3-DHBA in Fig. 3. The modified electrodes were stored at room temperature (ca. 20 $^{\circ}$C) in an air-tight container with silica beads supplied by vendor during intermittent use of the electrodes with HPLC (up to 45 days).

The reproducibility of stability achieved via FIA as shown in Fig. 4a was translated to HPLC experiments by repeating the injection of the 2,3-DHBA 5 times each on 3 different days (day 1, day 30, and day 45) and is illustrated in Fig. 4b. The resulting sensitivity 13.35 nA µM^{-1} (RSD 2.7%) shows the stability of ZrO$_2$-Au electrode was 45 days in the HPLC. The demonstrated stability of ZrO$_2$-Au electrode in a flow-based analytical platforms is the highest amongst the modified EC sensors reported [26, 27] to-date.

3.4 Real sample analysis

To demonstrate the applicability of the ZrO_2-Au electrode to real sample analysis, tap water from chemistry laboratory and river water samples obtained from the Derwent River (Hobart, Australia) were spiked with ascorbic acid, 2,3-DHBA, and pyrocatechol. Then, amperometric current of real samples at the ZrO_2-Au electrode in HPLC were recorded under optimized conditions. The results are summarized in Table 2 and the calculated recovery values were in the range of 98-102.5%. Therefore, the ZrO_2-Au electrode can be applied for practical and low-cost analysis of target solutes in water using flow-based analytical system.

Table 2. Determination of ascorbic acid, 2,3-DHBA, and pyrocatechol in real water samples (n= 3).

Solutes	Added [µM]	Tap water		River water	
		Found [µM]	Recovery [%]	Found [µM]	Recovery [%]
Ascorbic acid	0.5	0.49 ± 0.03	98	0.49 ± 0.03	98.7
	1	1 ± 0.03	99.6	1 ± 0.04	100.3
	5	5.07 ± 0.04	101.3	5.07 ± 0.03	101.5
2,3-DHBA	0.5	0.5 ± 0.03	99.3	0.5 ± 0.01	99.7
	1	1 ± 0.02	99.6	1.01 ± 0.02	100
	5	5.02 ± 0.04	100.4	5.04 ± 0.03	100.7
Pyrocatechol	0.5	0.49 ± 0.02	98.7	0.5 ± 0.01	100
	1	1.01 ± 0.02	100.7	1.02 ± 0.02	101.7
	5	5.09 ± 0.08	101.8	5.12 ± 0.03	102.5

4. Conclusions

In this study, a comprehensive EC characterisation of Au electrode with nanoparticulate ZrO_2 is investigated for flow-based analytical systems. Voltammograms show that ZrO_2-Au electrode provides faster electron transfer rates, with current and effective surface area increased by approx. 100% compared to the bare-Au, for enhanced redox abilities towards the test solute. We demonstrate the use of ZrO_2 NPs-modified electrodes for EC detection in flow-based analytical systems including HPLC and FIA for the first time. Using AD in HPLC, we obtained LOD values for the test solutes (2,3-DHBA, and pyrocatechol) which were approx. 2 times lower than reported LODs to-date. The results provided *ca.* 3 times reduction in baseline noise compared to previously reported EC detection. Moreover, the ZrO_2-Au electrode demonstrated good repeatability,

reproducibility, and stability for 8.5 hr in continuous-flow in FIA and 45 days during intermittent use with HPLC at flow rate of 0.6 mL min^{-1}.

Acknowledgements

5. References

[1] M. Steinhart, Introduction to nanotechnology. By Charles P. Poole, Jr. and Frank J. Owens, Angew. Chem. Int. Ed., 43 (2004) 2196-2197.

[2] X. Luo, A. Morrin, A.J. Killard, M.R. Smyth, Application of nanoparticles in electrochemical sensors and biosensors, Electroanalysis, 18 (2006) 319-326.

[3] J. Wang, Nanomaterial-based electrochemical biosensors, Analyst, 130 (2005) 421-426.

[4] G. March, T.D. Nguyen, B. Piro, Modified electrodes used for electrochemical detection of metal ions in environmental analysis, Biosensors, 5 (2015) 241-275.

[5] Z. Taleat, A. Khoshroo, M. Mazloum-Ardakani, Screen-printed electrodes for biosensing: a review (2008–2013), Microchim. Acta, 181 (2014) 865-891.

[6] V. Bhalla, S. Carrara, P. Sharma, Y. Nangia, C. Raman Suri, Gold nanoparticles mediated label-free capacitance detection of cardiac troponin I, Sensors Actuators B: Chem., 161 (2012) 761-768.

[7] G.A. Ruiz-Córdova, S. Khan, L.M. Gonçalves, M.I. Pividori, G. Picasso, T.S. Maria Del Pilar, Electrochemical sensing using magnetic molecularly imprinted polymer particles previously captured by a magneto-sensor, Talanta, 181 (2017) 19-23.

[8] E. Katz, I. Willner, J. Wang, Electroanalytical and bioelectroanalytical systems based on metal and semiconductor nanoparticles, Electroanalysis, 16 (2004) 19-44.

[9] M. Mazloum-Ardakani, A. Dehghani-Firouzabadi, N. Rajabzade, M.A. Sheikh-Mohseni, A. Benvidi, M. Abdollahi-Alibeik, MCM/ZrO_2 nanoparticles modified electrode for simultaneous and selective voltammetric determination of epinephrine and acetaminophen, J. Iran. Chem. Soc., 10 (2013) 1-5.

[10] S.E.F. Kleijn, S.C.S. Lai, M.T.M. Koper, P.R. Unwin, Electrochemistry of nanoparticles, Angew. Chem. Int. Ed., 53 (2014) 3558-3586.

[11] M.A. Islam, P. Mahbub, P.N. Nesterenko, B. Paull, M. Macka, Prospects of pulsed amperometric detection in flow-based analytical systems - A review, Anal. Chim. Acta, 1052 (2019) 10-26.

[12] M.A. Islam, S.C. Lam, Y. Li, M.A. Atia, P. Mahbub, P.N. Nesterenko, B. Paull, M. Macka, Capillary gap flow cell as capillary-end electrochemical detector in flow-based analysis, Electrochim. Acta, 303 (2019) 85-93.

[13] C. Wang, J. Du, H. Wang, C.e. Zou, F. Jiang, P. Yang, Y. Du, A facile electrochemical sensor based on reduced graphene oxide and Au nanoplates modified glassy carbon electrode for simultaneous detection of ascorbic acid, dopamine and uric acid, Sensors Actuators B: Chem., 204 (2014) 302-309.

[14] V. Carralero, A. González-Cortés, P. Yáñez-Sedeño, J. Pingarron, Pulsed amperometric detection of histamine at glassy carbon electrodes modified with gold nanoparticles, Electroanalysis, 17 (2005) 289-297.

[15] G.C. Sedenho, J.L. da Silva, M.A. Beluomini, A.C. de Sá, N.R. Stradiotto, Determination of electroactive organic acids in sugarcane vinasse by high performance anion-exchange chromatography with pulsed amperometric detection using a nickel nanoparticle modified boron-doped diamond, Energy Fuels, 31 (2017) 2865-2870.

[16] J.L. da Silva, M.A. Beluomini, N.R. Stradiotto, Determination of furanic aldehydes in sugarcane bagasse by high-performance liquid chromatography with pulsed amperometric detection using a modified electrode with nickel nanoparticles, J. Sep. Sci., 38 (2015) 3176-3182.

[17] R.A. Medeiros, B.C. Lourencao, R.C. Rocha-Filho, O. Fatibello-Filho, Flow injection simultaneous determination of synthetic colorants in food using multiple pulse amperometric detection with a boron-doped diamond electrode, Talanta, 99 (2012) 883-889.

[18] T. de Jesus Guedes, G. Antônio Reis Andrade, A. Barbosa Lima, R. Amorim Bezerra da Silva, W. Torres Pio dos Santos, Simple and fast determination of warfarin in pharmaceutical samples using boron-doped diamond electrode in bia and fia systems with multiple pulse amperometric detection, Electroanalysis, 29 (2017) 2340-2347.

[19] C. Karuwan, T. Mantim, P. Chaisuwan, P. Wilairat, K. Grudpan, P. Jittangprasert, Y. Einaga, O. Chailapakul, L. Suntornsuk, O. Anurukvorakun, Pulsed amperometry for anti-fouling of boron-doped diamond in electroanalysis of β-agonists: application to flow injection for pharmaceutical analysis, Sensors, 6 (2006) 1837-1850.

[20] T. Peik-See, A. Pandikumar, H. Nay-Ming, L. Hong-Ngee, Y. Sulaiman, Simultaneous electrochemical detection of dopamine and ascorbic acid using an iron oxide/reduced graphene oxide modified glassy carbon electrode, Sensors, 14 (2014) 15227-15243.

[21] Periodic table technical data, Wolfram Research Inc., http://periodictable.com/Elements/079/data.wt.html (accessed July 2018).

[22] R.A.S. Couto, J.L.F.C. Lima, M.B. Quinaz, Recent developments, characteristics and potential applications of screen-printed electrodes in pharmaceutical and biological analysis, Talanta, 146 (2016) 801-814.

[23] S.-W. Ui, I.-S. Choi, S.-C. Choi, Synthesis of high surface area mesoporous silica powder using anionic surfactant, ISRN Materials Science, 2014 (2014) 1-6.

[24] S.Z. Mohammadi, H. Beitollahi, E.B. Asadi, Electrochemical determination of hydrazine using a ZrO_2 nanoparticles-modified carbon paste electrode, Environ. Monit. Assess., 187 (2015) 122.

[25] P.K.Q. Nguyen, Cyclic voltammetric and square wave anodic stripping voltammetric analysis of lead and cadmium utilizing the novel titanium dioxide/zirconium dioxide/tween 80 carbon paste composite electrode, Wright State University, Dayton, USA, 2013, pp. 1-160.

[26] V.P. Hanko, J.S. Rohrer, Determination of tobramycin and impurities using high-performance anion exchange chromatography with integrated pulsed amperometric detection, J. Pharm. Biomed. Anal., 40 (2006) 1006-1012.

[27] J. Cheng, P. Jandik, N. Avdalovic, Pulsed amperometric detection of sulfide, cyanide, iodide, thiosulfate, bromide and thiocyanate with microfabricated disposable silver working electrodes in ion chromatography, Anal. Chim. Acta, 536 (2005) 267-274.

[28] N. Mohammadizadeh, S.Z. Mohammadi, M. Kaykhaii, Highly sensitive amperometric detection of propranolol using graphite screen printed electrode modified with zirconium dioxide nanoparticles, Anal. Bioanal. Electrochem., 9 (2017) 277-285.

[29] P.K.Q. Nguyen, S.K. Lunsford, Electrochemical response of carbon paste electrode modified with mixture of titanium dioxide/zirconium dioxide in the detection of heavy metals: Lead and cadmium, Talanta, 101 (2012) 110-121.

[30] N.M. Ahmad, J. Abdullah, N.A. Yusof, A.H. Ab Rashid, S. Abd Rahman, M.R. Hasan, Amperometric biosensor based on zirconium oxide/polyethylene glycol/tyrosinase composite film for the detection of phenolic compounds, Biosensors, 6 (2016) 31-44.

[31] Y. Zhang, X. Chen, W. Yang, Direct electrochemistry and electrocatalysis of myoglobin immobilized in zirconium phosphate nanosheets film, Sensors Actuators B: Chem., 130 (2008) 682-688.

[32] I.A. Rutkowska, A. Wadas, P.J. Kulesza, Mixed layered WO_3/ZrO_2 films (with and without rhodium) as active supports for PtRu nanoparticles: enhancement of oxidation of ethanol, Electrochim. Acta, 210 (2016) 575-587.

[33] G.K. Sidhu, R. Kumar, Role of anionic and cationic surfactants on the structural and dielectric properties of ZrO_2 nanoparticles, Appl. Surf. Sci., 392 (2017) 598-607.

[34] D.C. Harris, Quantitative chemical analysis, Seventh ed., W. H. Freeman and Company, New York, 2007.

[35] J. Li, Y. Hu, P.W. Carr, Fast separations at elevated temperatures on polybutadiene-coated zirconia reversed-phase material, Anal. Chem., 69 (1997) 3884-3888.

[36] H. Karimi-Maleh, M. Moazampour, A.A. Ensafi, S. Mallakpour, M. Hatami, An electrochemical nanocomposite modified carbon paste electrode as a sensor for simultaneous determination of hydrazine and phenol in water and wastewater samples, Environ. Sci. Pollut. Res., 21 (2014) 5879-5888.

[37] I.M. Ibrahim, M.E. Moustafa, M.R. Abdelhamid, Effect of organic acids precursors on the morphology and size of ZrO_2 nanoparticles for photocatalytic degradation of Orange G dye from aqueous solutions, J. Mol. Liq., 223 (2016) 741-748.

[38] M.B. Gholivand, A. Azadbakht, A novel hydrazine electrochemical sensor based on a zirconium hexacyanoferrate film-bimetallic Au–Pt inorganic–organic hybrid nanocomposite onto glassy carbon-modified electrode, Electrochim. Acta, 56 (2011) 10044-10054.

[39] M. Li, Y.-T. Li, D.-W. Li, Y.-T. Long, Recent developments and applications of screen-printed electrodes in environmental assays—A review, Anal. Chim. Acta, 734 (2012) 31-44.

[40] Voltammetric methods, Electrochemical methods, LibreTexts libraries, The California State University
https://chem.libretexts.org/LibreTexts/Northeastern/11%3A_Electrochemical_Methods/11.4%3A_Voltammetric_Methods (01.04.2019).

[41] Z. Nie, C.A. Nijhuis, J. Gong, X. Chen, A. Kumachev, A.W. Martinez, M. Narovlyansky, G.M. Whitesides, Electrochemical sensing in paper-based microfluidic devices, Lab Chip, 10 (2010) 477-483.

[42] P.J. O'Connell, C. Gormally, M. Pravda, G.G. Guilbault, Development of an amperometric l-ascorbic acid (Vitamin C) sensor based on electropolymerised aniline for pharmaceutical and food analysis, Anal. Chim. Acta, 431 (2001) 239-247.

[43] 2,3-Dihydroxybenzoic acid, National Centre for Biotechnology Information, U.S. National Library of Medicine, Rockville Pike, USA.

[44] Pyrocatechol, National Center for Biotechnology Information, U.S. National Library of Medicine, Rockville Pike, USA.

[45] Y. Li, M. Dvorak, P.N. Nesterenko, R. Stanley, N. Nuchtavorn, L.K. Krcmova, J. Aufartova, M. Macka, Miniaturised medium pressure capillary liquid chromatography system with flexible open platform design using off-the-shelf microfluidic components, Anal. Chim. Acta, 896 (2015) 166-176.

[46] C.-c. Jiang, Y.-k. Cao, G.-y. Xiao, R.-f. Zhu, Y.-p. Lu, A review on the application of inorganic nanoparticles in chemical surface coatings on metallic substrates, RSC Advances, 7 (2017) 7531-7539.

[47] L. Ghasemi-Mobarakeh, D. Semnani, M. Morshed, A novel method for porosity measurement of various surface layers of nanofibers mat using image analysis for tissue engineering applications, J. Appl. Polym. Sci., 106 (2007) 2536-2542.

[48] W. He, Z. Ma, T. Yong, W.E. Teo, S. Ramakrishna, Fabrication of collagen-coated biodegradable polymer nanofiber mesh and its potential for endothelial cells growth, Biomaterials, 26 (2005) 7606-7615.

[49] G.R. Blake, Particle density, in: W. Chesworth (Ed.) Encyclopedia of Soil Science, Springer Netherlands, Dordrecht, 2008, pp. 504-505.

[50] Zirconium oxide nanopowder, US Research Nanomaterials Inc., Houston, TX 77084, USA.

[51] N. Elgrishi, K.J. Rountree, B.D. McCarthy, E.S. Rountree, T.T. Eisenhart, J.L. Dempsey, A Practical Beginner's Guide to Cyclic Voltammetry, J. Chem. Educ., 95 (2018) 197-206.

[52] V. Fragkou, Y. Ge, G. Steiner, D. Freeman, N. Bartetzko, A.P. Turner, Determination of the real surface area of a screen-printed electrode by chronocoulometry, Int. J. Electrochem. Sci, 7 (2012) 6214-6220.

[53] S. Trasatti, O.A. Petrii, Real surface area measurements in electrochemistry, J. Electroanal. Chem., 327 (1992) 353-376.

[54] D. Sawyer, W. Heineman, J. Beebe, Chemistry experiments for instrumental analysis, John Wiley & Sons, Inc., New York, 1984.

[55] J. Moldenhauer, M. Meier, D.W. Paul, Rapid and direct determination of diffusion coefficients using microelectrode arrays, J. Electrochem. Soc., 163 (2016) H672-H678.

[56] J. Krejci, Z. Sajdlova, V. Nedela, E. Flodrova, R. Sejnohova, H. Vranova, R. Plicka, Effective surface area of electrochemical sensors, J. Electrochem. Soc., 161 (2014) B147-B150.

[57] Y. Lin, H. Zhao, F. Yu, J. Yang, Design of an Extended Experiment with Electrical Double Layer Capacitors: Electrochemical Energy Storage Devices in Green Chemistry, Sustainability, 10 (2018) 3630-3638.

[58] T. Charoenraks, S. Palaharn, K. Grudpan, W. Siangproh, O. Chailapakul, Flow injection analysis of doxycycline or chlortetracycline in pharmaceutical formulations with pulsed amperometric detection, Talanta, 64 (2004) 1247-1252.

[59] L.M. Da Silva, L.A. De Faria, J.F.C. Boodts, Determination of the morphology factor of oxide layers, Electrochim. Acta, 47 (2001) 395-403.

[60] C. Lämmel, M. Schneider, M. Weiser, A. Michaelis, Investigations of electrochemical double layer capacitor (EDLC) materials – a comparison of test methods, Materialwiss. Werkstofftech., 44 (2013) 641-649.

[61] T. Pluangklang, J.B. Wydallis, D.M. Cate, D. Nacapricha, C.S. Henry, A simple microfluidic electrochemical HPLC detector for quantifying Fenton reactivity from welding fumes, Anal. Methods, 6 (2014) 8180-8186.

[62] K. Štulík, V. Pacáková, Electrochemical detection in HPLC. Part. 1. Principles, techniques and instrumentation, Food / Nahrung, 29 (1985) 501-516.

[63] M. Trojanowicz, Recent developments in electrochemical flow detections—a review: Part ii. Liquid chromatography, Anal. Chim. Acta, 688 (2011) 8-35.

[64] J. Fedorowski, W.R. LaCourse, A review of pulsed electrochemical detection following liquid chromatography and capillary electrophoresis, Anal. Chim. Acta, 861 (2015) 1-11.